www.czasopisma.pan.pl PAN www.journals.pan.pl

ARCHIVES of FOUNDRY ENGINEERING

ISSN (2299-2944)
Volume 18
Issue 1/2018

115 – 118

21/1

DOI: 10.24425/118822

Published quarterly as the organ of the Foundry Commission of the Polish Academy of Sciences

Analysis of Temperature and Velocity Fields During Filling of Continuous Casting Mould

L. Sowa *, T. Skrzypczak, P. Kwiatoń
Institute of Mechanics and Machine Design Fundamentals, Częstochowa University of Technology
Dąbrowskiego 73, 42-200 Częstochowa, Poland
*Corresponding author. E-mail address: sowa@imipkm.pcz.pl

Received 04.07.2017; accepted in revised form 19.08.2017

Abstract

In this paper, the mathematical model and numerical simulations of the molten steel flow by the submerged entry nozzle and the filling process of the continuous casting mould cavity are presented. In the mathematical model, the temperature fields were obtained by solving the energy equation, while the velocity fields were calculated by solving the momentum equations and the continuity equation. These equations contain the turbulent viscosity which is found by solving two additional transport equations for the turbulent kinetic energy and its rate of dissipation. In the numerical simulations, coupling of the thermal and fluid flow phenomena by changes in the thermophysical parameters of alloy depending on the temperature has been taken into consideration. This problem (2D) was solved by using the finite element method. Numerical simulations of filling the continuous casting mould cavity were performed for two variants of liquid metal pouring. The effect of the cases of pouring the continuous casting mould on the velocity fields and the solid phase growth kinetics in the process of filling the continuous casting mould was evaluated as these magnitudes have an influence on the high quality of the continuous cast steel slab.

Keywords: Solidification process, Continuous casting, Numerical simulation, Molten metal flow

1. Introduction

Nowadays, the continuous casting process is well widespread as the standard process of the production slabs in most steelmaking plants. This process has been developed intensively in recent years because it has better efficiency and heat effectiveness than casting to ingot moulds [1, 2]. The large number of phenomena in the process of continuous steel casting (CSC), especially great-size cast slabs, extorts a need for continuous research of this process. Due to high costs of empirical researches, the mathematical modelling is becoming an important tool for analyzing the thermal-flow phenomena of the CSC process. So there is a need to formulate conjugate mathematical models that take into account these phenomena [1 - 6]. When analyzing liquid metal movements in the continuous casting mould, the appropriate type of submerged entry nozzle is of great importance. This enables controlling the flow of liquid steel, allowing the separation of non-metallic inclusions and transporting them to the slag layer [1, 4, 5]. The purpose of this paper is to estimate the influence of liquid metal motion and pouring manners (two types of submerged entry nozzle) on velocity fields and the kinetics of solid phase growth in the rectangular cast slab at the initial stage of CSC process. These actions are aimed at improving the strength properties of the steel.

2. Mathematical description

The mathematical model of liquid metal flow within the continuous casting mould cavity during the filling has been

proposed. It was assumed that the solidification front is mushy [4 - 7]. The mathematical model is based on the solution of the following system of differential equations (the energy equation, the momentum equations and continuity equation) [1, 5]:

$$\rho C_{ef}\left(\frac{\partial T}{\partial t}+v_j\frac{\partial T}{\partial x_j}\right)=\frac{\partial}{\partial x_j}\left(\lambda\frac{\partial T}{\partial x_j}+\frac{c\mu_t}{\sigma_t}\frac{\partial T}{\partial x_j}\right), \tag{1}$$

$$\rho\left(\frac{\partial v_i}{\partial t}+v_j\frac{\partial v_i}{\partial x_j}\right)=\frac{\partial}{\partial x_j}\left((\mu+\mu_t)\left(\frac{\partial v_i}{\partial x_j}+\frac{\partial v_j}{\partial x_i}\right)-\frac{2}{3}\rho k\delta_{ij}\right)-\frac{\partial p}{\partial x_i}+\rho g_i, \tag{2}$$

$$\frac{\partial v_j}{\partial x_j}=0, \tag{3}$$

Occurring in (1) and (2), the turbulence dynamical viscosity coefficient (μ_t) is defined as follows:

$$\mu_t=c_\mu\rho\frac{k^2}{\varepsilon}, \tag{4}$$

In the above formula, k and ε are obtained from the following equations (the equation for turbulence kinetic energy and equation for dissipation rate of turbulence kinetic energy) [5, 6]:

$$\rho\left(\frac{\partial k}{\partial t}+v_j\frac{\partial k}{\partial x_j}\right)=\frac{\partial}{\partial x_j}\left((\mu+\frac{\mu_t}{\sigma_k})\frac{\partial k}{\partial x_j}\right)+\mu_t\frac{\partial v_i}{\partial x_j}\left(\frac{\partial v_i}{\partial x_j}+\frac{\partial v_j}{\partial x_i}\right)-\frac{\mu_t}{\rho\sigma_\rho}\frac{\partial\rho}{\partial x_i}g_i-\rho\varepsilon, \tag{5}$$

$$\rho\left(\frac{\partial\varepsilon}{\partial t}+v_j\frac{\partial\varepsilon}{\partial x_j}\right)=\frac{\partial}{\partial x_j}\left((\mu+\frac{\mu_t}{\sigma_\varepsilon})\frac{\partial\varepsilon}{\partial x_j}\right)-c_2\rho\frac{\varepsilon^2}{k}+c_1\frac{\varepsilon}{k}\mu_t\frac{\partial v_i}{\partial x_j}\left(\frac{\partial v_i}{\partial x_j}+\frac{\partial v_j}{\partial x_i}\right)-c_1(1-c_3)\frac{\varepsilon}{k}\frac{\mu_t}{\rho\sigma_\rho}\frac{\partial\rho}{\partial x_i}g_i, \tag{6}$$

where: T – the temperature [K], λ – the thermal conductivity coefficient [W/(mK)], v_j – the velocity vector of liquid metal flow [m/s], p – the pressure [N/m^2], $\rho=\rho(T)$ – the density [kg/m^3], $C_{ef}(T)=c_{LS}+L/(T_L-T_S)$ – the effective specific heat of a mushy zone [J/(kgK)] [4, 7], c_{LS} – the specific heat of a mushy zone [J/(kgK)], L – the latent heat of solidification [J/kg], $\mu(T)$ – the dynamical viscosity coefficient [Ns/m^2], c – the specific heat [J/(kgK)], T_L, T_S - the temperature of liquidus and solidus line, respectively [K], g_i – the vector of the gravity acceleration [m/s^2], μ_t – the turbulence dynamical viscosity coefficient [Ns/m^2], k – the turbulence kinetic energy [m^2/s^2], ε - the dissipation rate of turbulence kinetic energy [m^2/s^3], t – time [s], x_j – the coordinates of vector of a node's position [m], $\sigma_t = 0.9$, $\sigma_\varepsilon = 1.3$, $\sigma_p = 0.9$, $c_1 = 1.44$, $c_2 = 1.92$, $c_3 = 0.8$, $c_\mu = 0.09$, σ_k=1 - empirical constants [5, 6]

The system of equations (1 - 6) is completed by the initial conditions and appropriate boundary conditions which are shown in Figure 1 [4 - 7]. For the equations (4 - 6), the zero value k and ε on the walls of continuous casting mould was assumed [5, 6].

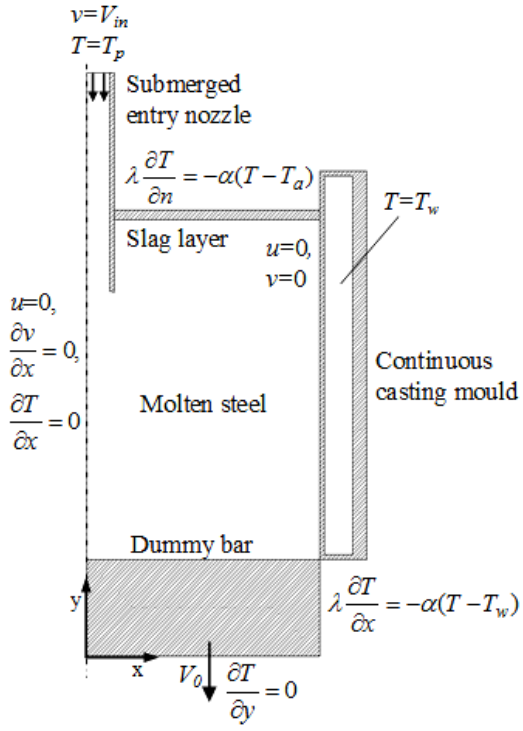

Fig. 1. Schematic illustration of the continuous casting mould containing boundary conditions

The above problem was solved by using the finite element method in the weighted residuals formulation [4, 7]. In numerical simulations, the Fidap program was used because it allows simulation of the flow of liquid metal at high speeds and ensures the rapid convergence of numerical solution.

3. Example of numerical calculations

The calculations were performed for the continuous casting mould with the rectangular cross-section cavity 0.3x1 m and length 0.8 m. The superheated steel with temperature $T_p = 1850$ K was poured with velocity $V_{in} = 0.38$ and 0.2 m/s into the considered region with the initial temperature $T_M = 500$ K. The thermophysical properties of a cast steel were taken from works [3 - 5, 7, 8]. The characteristic temperatures of liquid steel were equal to: $T_L = 1810$ K, $T_S = 1760$ K, whereas the ambient and cooling water temperature amounted to $T_a = 303$ K, $T_w = 288$ K, respectively. The heat-transfer coefficient (α) between the continuous casting mould and ambient was equal $\alpha_m = 50$ W/(m^{2}K) and between the slag and ambient $\alpha_s = 3$ W/(m^{2}K) [4, 8]. The thermal and fluid flow phenomena occurring in the considered system were analyzed. The selected results of numerical simulations are shown in Figures 2 - 4. The filling process of the continuous casting mould cavity was

performed for two cases of liquid metal pouring: the vertical (I variant) (Figs 2, 3) and horizontal (II variant) (Fig. 4).

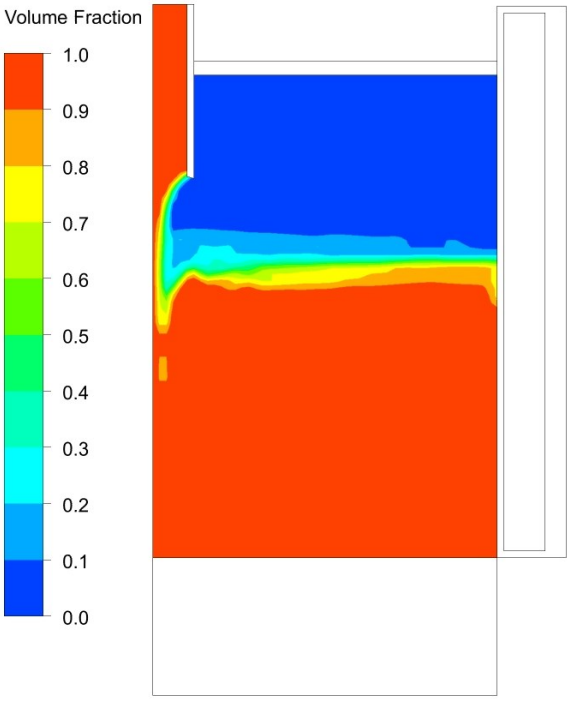

Fig. 2. The state of filling of the continuous casting mould cavity at time t=12 s, I variant

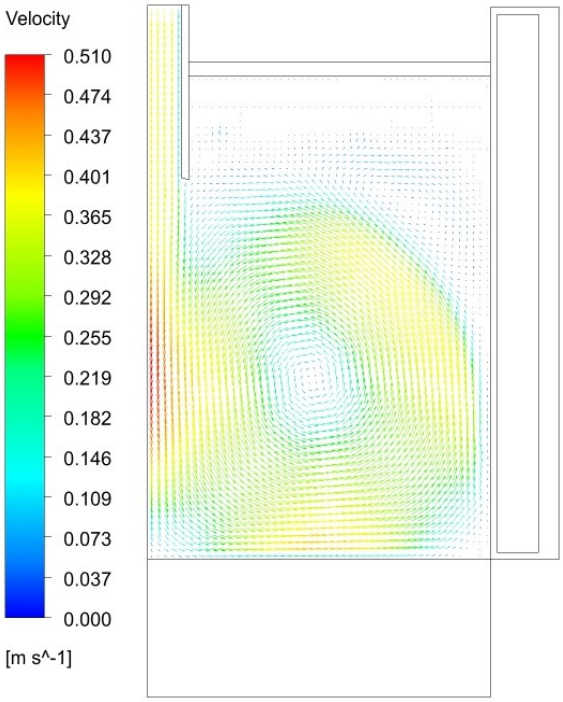

Fig. 3. Velocity field after filling of the continuous casting mould at time t=20 s, I variant

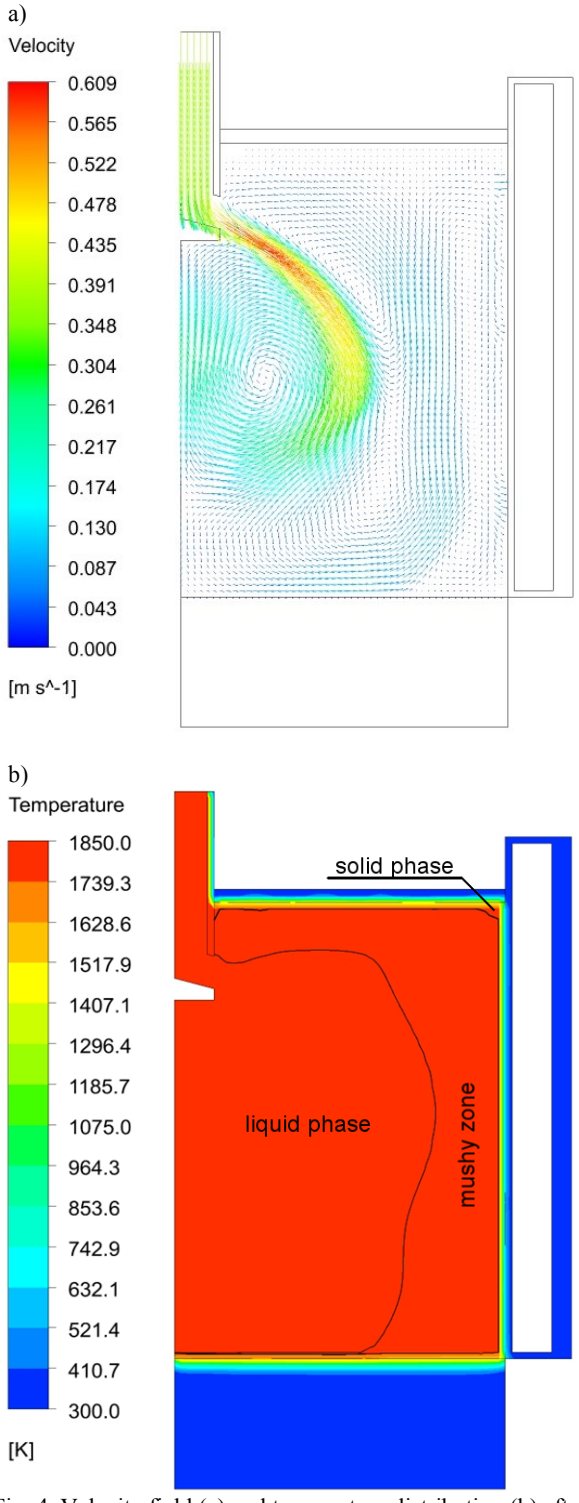

Fig. 4. Velocity field (a) and temperature distribution (b) after time t=20 s, II variant

4. Conclusions

This paper focuses mainly on the analysis of thermal and fluid flow phenomena occurring in the continuous casting mould at the initial stage of CSC process. The effect of the case of pouring the continuous casting mould onto the liquid phase velocity fields and the kinetics of solid phase growth in the cast slab was evaluated. Results of numerical simulation are presented in the form of temperature and velocity fields (Figs 2-4). The liquidus and solidus lines are visible on the temperature field presented in Figure 4b. They indicate the current position of the two-phase zone, while the solidus line indicates the instantaneous thickness of the solid phase. It has been observed that in the case of vertical and horizontal pouring there are no significant differences in the thickness and shape of the solid phase formed on the walls of the continuous casting mould. This conclusion applies only to the filling period of the continuous casting mould (time 20 s, Figs 3, 4). Additionally, it is noted that at the assumed pouring velocity, the thickness of the solidified layer formed is insufficient to start the next step of continuous casting and therefore the pouring velocity must be reduced. Currently, the continuous casting mould is not only an element of a continuous casting machine in which cast slabs are formed, but it becomes an additional place where the steel cleaning from non-metallic inclusions is performed. Researches of inclusions separation process at the industrial plant are nearly impossible because of the lack of optical accessibility and high temperature inside the continuous casting mould. For this reason the numerical simulations are becoming an important tool to analyze all phenomena of the continuous casting process. Performing the operation of removing inclusions requires an appropriate targeted movement of the liquid metal towards the slag layer. Such liquid metal movements are achieved by a suitably directed outflow from the submerged entry nozzles, which is associated with the cases of pouring the liquid metal to the continuous casting mould. (cf Fig. 3 and 4a). Numerical studies on the velocity distribution in continuous casting mould show that the flow field generated by horizontal outflow nozzles is more favourable to the removal of inclusions. The change in the distribution of non-metallic inclusions in the continuous casting mould has the significant effect on the surface state and mechanical properties of the obtained cast slab.

References

[1] Zhao, B., Thomas, B.G., Vanka, S.P. & Omalley, R.J. (2005). Transient fluid flow and superheat transport in continuous casting of steel slabs. *Metallurgical and Materials Transactions B*. 36, 801-823. DOI: 10.1007/s11663-005-0083-3.

[2] Szajnar, J., Stawarz, M., Wróbel, T., Sebzda, W., Grzesik, B. & Stępień, M. (2010). Influence of continuous casting conditions on grey cast iron structure. *Archives of Materials Science and Engineering*. 42(1), 45-52.

[3] Burbelko, A., Fallus, J., Kapturkiewicz, W., Sołek, K., Drożdż, P. & Wróbel, M. (2012). Modeling of the grain structure formation in the steel continuous ingot by CAFE method. *Archives of Metallurgy and Materials*. 57(1), 379-384. DOI: 10.2478/v10172-012-0037-0.

[4] Sowa, L. (2011). Effect of nozzle outlet angle on flow and temperature field in a slab continuous casting mould. *Archives of Foundry Engineering*. 11(2), 199-202.

[5] Lei, S., Zhang, J., Zhao, X. & He, K. (2014). Numerical simulation of molten steel flow and inclusions motion behavior in the solidification processes for continuous casting slab. *ISIJ Int*. 54(1), 94-102. DOI: org/10.2355/isijinternational.54.94.

[6] Liu, Z., Li, L., Qi, F., Li, B., Jiang, M. & Tsukihashi F. (2015). Population balance modeling of polydispersed bubbly flow in continuous-casting using multiple-size-group approach. *Metallurgical and Materials Transactions B*. 46(1), 406-420. DOI:10.1007/s11663-014-0192-y.

[7] Węgrzyn-Skrzypczak, E. & Skrzypczak, T. (2014). Mathematical and numerical basis of binary alloy solidification models with substitute thermal capacity. Part II. *Journal of Applied Mathematics and Computational Mechanics*. 13(2), 141-147.

[8] Miłkowska-Piszczek, K & Korolczuk-Hejnak, M. (2013). An analysis of the influence of viscosity on the numerical simulation of temperature distribution as demonstrated by the CC process. *Archives of Metallurgy and Materials*. 58(4), 1267-1274. DOI: 10.2478/amm-2013-0146.